Sensors & Actuators: B. Chemical 368 (2022) 132209

Contents lists available at ScienceDirect

Sensors and Actuators: B. Chemical

journal homepage: www.elsevier.com/locate/snb

Detection of gingipain activity using solid state nanopore sensors

Quentin Palomar [a], Anna Svärd [b,c], Shuangshuang Zeng [a], Qitao Hu [a], Funing Liu [a], Daniel Aili [b,*], Zhen Zhang [a,*]

[a] Division of Solid-State Electronics, Department of Electrical Engineering, The Ångström Laboratory, Uppsala University, P.O. Box 534, SE-751 21 Uppsala, Sweden
[b] Cardiovascular Research Centre (CVRC), School of Medical Sciences, Örebro University, SE-781 82 Örebro, Sweden
[c] Laboratory of Molecular Materials, Division of Biophysics and Bioengineering, Department of Physics, Chemistry and Biology (IFM), Linköping University, SE-581 83 Linköping, Sweden

ARTICLE INFO

Keywords:
Biosensor
Solid-state nanopore
Pore blocking
Pore opening
Trypsin
Enzyme detection
Gingipains

ABSTRACT

Accurate, robust, and rapid diagnostics is the basis for all well-functioning healthcare. There is a large need in point-of-care biosensors to facilitate diagnosis and reduce the need for cumbersome laboratory equipment. Proteases are key virulence factors in periodontitis. Periodontal disease is very common and characterized by inflammation and infection in the tooth-supporting structures and is linked to many systemic diseases such as cardiovascular disease, diabetes, and Alzheimer's disease. Proteases present in periodontal disease, gingipains, are highly responsible for the disease onset and progression and are therefore a promising biomarker. Here we show a novel nanopore-based biosensor strategy for protease activity monitoring. Solid-state nanopores were modified with a proteolytic substrate, restricting the ionic current through the apertures of the nanopores. Protease can digest the proteolytic substrate thus enlarge the aperture and the ionic current. Trypsin was used as an initial model protease to investigate the performance of the sensor. We show that the solid-state nanopore-biosensor can detect trypsin with a limit of detection (LOD) of 0.005 ng/mL (0.2 pM). The detection system developed for the model enzyme was then applied to the detection of gingipains. The LOD for detection of gingipains was 1 ng/mL (0.02 nM), with a 27% recovery of the signal at 0.1 μg/mL, indicating that the sensitivity and dynamic range are relevant for the clinical diagnosis of periodontitis. The generic detection of protease activity and high sensitivity make this a promising sensor technology for both diagnosis of periodontal disease and monitoring of other disease-related proteases.

1. Introduction

Endogenous proteolytic enzymes are overexpressed in numerous diseases, including cancer and autoimmune diseases. Bacterial infections are also typically resulting in upregulated protease activity as consequence of both the host-response reactions and pathogen expression of proteases. Proteases are thus highly relevant diagnostic and prognostic biomarkers, and interesting drug targets. Regulation of protease activity is, however, often very complex. Assays and sensors for detection of protease activity can provide better assessment of disease progression compared to detection of protease abundance alone. Development of generic strategies for activity-based diagnostics is challenging. Fluorescence-based protease assays are most popular in laboratory pre-clinical settings due to high sensitivity, but there are difficulties with stability of fluorescent molecules and the possibilities to perform point-of care testing are scarce. Colorimetric assays exploiting gold nanoparticles (AuNPs) are simple, however, functionalization must be carefully optimized. Electrochemical protease activity sensors are promising due to high sensitivity and possibilities to miniaturize, but more studies are still needed for development of this approach in further applications [1].

Periodontitis is a disease that includes inflammation and infection of tooth-supporting tissues, eventually leading to tooth-loss [2]. The disease is very common, affecting approximately 50% of the adult population [3]. The inflammation and infection are not limited to only the oral cavity, pathogens and markers for periodontitis have been found in various tissues in the body, among others in the atherosclerotic plaque [4] and recently, in brain tissue [5]. The disease is associated with many systemic diseases where the most studied interactions are with cardiovascular disease [6], diabetes [7], and Alzheimer's disease [8]. *Porhyromonas gingivalis* (*P. gingivalis)* is a key-pathogen in periodontitis that secretes gingipain enzymes, which are well-studied and highly

* Corresponding authors.
E-mail addresses: daniel.aili@liu.se (D. Aili), zhen.zhang@angstrom.uu.se (Z. Zhang).

https://doi.org/10.1016/j.snb.2022.132209
Received 13 March 2022; Received in revised form 8 June 2022; Accepted 10 June 2022
Available online 13 June 2022

responsible for the initiation and progression of the disease [9], thus making it an excellent candidate for a biomarker for not only the disease diagnostics but also for predicting disease activity. Knowing the activity of the disease would improve possibilities to set more accurate and individualized treatment plans, optimize care on-site in dental clinics, and facilitate daily maintenance by patients. Gingipain enzymes are cysteine-proteases, specific for either arginine (Rgp-subtype) or lysine (Kgp-subtype). Gingipains have multiple functionalities including degradation of bone tissue, promoting cell-to-cell communication, providing nutrients for their host bacteria etc. These proteases act in favor for the growth of their host bacteria *P. gingivalis* in many ways and is one of the most well-known components driving the disease progression [10].

Biosensors offers new means for rapid, accessible and cost-effective diagnostic of diseases, including periodontal disease [11]. Nanopore-based biosensors is currently mostly used for DNA sequencing and for the detection of biomolecules based on biological nanopores [12]. However, recent research has taken an interest on solid-state nanopores for the label-free and amplification-free detection of different bioanalytes [13]. Compared to biological nanopores, the geometry and chemical composition of solid-state nanopores can be tailored to meet different requirements and allow for use of specific surface chemistries and biorecognition strategies, providing advantages in terms of lifetime, mechanical robustness and chemical stability [14]. Another advantage of solid-state nanopores is the possibilities for device mass-production, which can facilitate fabrication of large quantities of instruments with identical performance. These sensing systems are also compatible with electronic and optical read-out technologies [15]. Chemical functionalization and immobilization of relevant biological or biomimetic receptors further enable specific biorecognition. The high sensitivities typically seen in nanopore-based sensors combined with small sample volumes [16], can further facilitate development of analytical methods for clinical settings, including detection of disease biomarkers in gingival crevicular fluid samples from periodontal pockets.

Here were show the development of a novel label-free, ultrasensitive silicon nanopore sensor for protease activity monitoring that can detect gingipain activity at clinically relevant concentrations. As illustrated in Fig. 1 A, the silicon nanopores have a truncated pyramidal shape [17] and the opening region of the nanopore was coated with a layer of gold to allow simple and efficient surface functionalization. Using thiol chemistry and appropriate linkers, selective immobilization of protease substrates (casein) inside the nanopore cavity could be performed. This resulted in a blocking of the nanopore opening, creating a dramatic drop in ion current. Upon proteolytic degradation of the immobilized casein, the obstructed nanopore was reopened. By measuring the ionic current though the nanopore, the changes in the aperture induced by both the protein immobilization and the proteolytic degradation could be

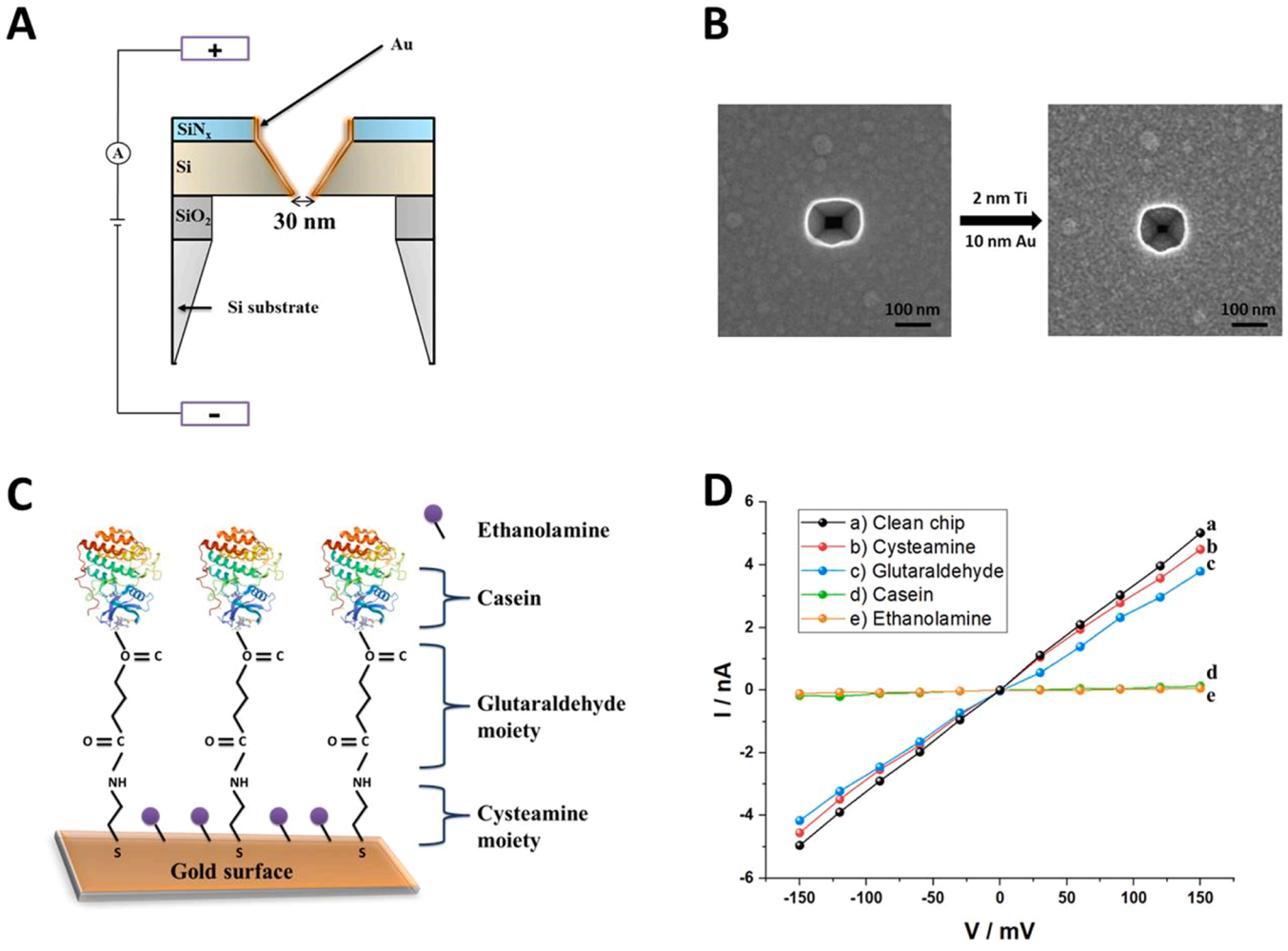

Fig. 1. A) Schematic representation of the structure of the nanopore. B) Top-view SEM images of the Si nanopore before and after deposition of Ti/Au layer at a magnification of × 400. C) Schematic representation of the composition of the molecular assembly on the surface of the nanopore after chemical modification. The multilayer consists firstly of cysteamine followed by glutaraldehyde, which serve as a link for the immobilization of casein, the last modification by ethanolamine limits non-specific adsorption. D) Current−Voltage characteristics at each stage of the chemical modification in 100 mM KCl.

monitored [18]. The sensor performance for detection of proteolytic activity was first investigated using trypsin as a model system (Fig. 1 C). Trypsin readily digest casein, resulting in a significant decrease in the overall size of the protein [19]. The catalytic mechanism of trypsin is closely related to gingipains, which play a key role in periodontal progression and disease outcome [20]. After optimization of the sensor using trypsin, we demonstrated the possibility to also detect gingipain activity in a more complex environment at clinically relevant concentrations. The demonstrated gingipain sensing could facilitate further development of low-cost chair-side sensors for rapid diagnostics of periodontal disease.

2. Experimental section

2.1. Chemicals and materials

Potassium chloride (KCl), cysteamine ($NH_2CH_2CH_2SH$), glutaraldehyde 50% solution ($OHC(CH_2)_3CHO$), ethanolamine (C_2H_7NO), Dithiothréitol ($C_4H_{10}O_2S_2$), polydimethylsiloxane (PDMS), Bovine serum albumin (BSA), Tris-buffered saline (TBS), phosphate-buffered saline (PBS), urea, cysteine, casein from bovine milk and trypsin from bovine pancreas were all purchased from Merck KGaA-Sigma-Aldrich, Darmstadt, Germany. The gingipain enzymes (GingisREX) were obtained from Genovis, Lund, Sweden. Spherical citrate covered AuNPs were purchased from BBI solutions, USA. All chemicals were used as received without any further purification. Water was supplied by the nanopure water system.

2.2. Instruments and characterization

Cleaning using O_2 plasma was performed in a Tepla 300 plasma processor (PVA TePla, Germany). Scanning electron microscopy (SEM) images were captured with Zeiss 6 LEO 1530 (Germany). UV−vis absorbance scans 400 − 800 nm was measured using an Infinite M1000PRO plate reader. Ellipsometry was performed with a Rudolph Research AutoEL III ellipsometer. For electrical measurements, the nanopore chip was placed between two liquid containers to form a flow cell. Once sealed by two PDMS O-rings (5 mm diameter) on the top and bottom side of the chip, the cell was filled with 100 mM KCl solution. Voltage was applied via two Ag/AgCl electrodes on both sides of the chip, thus allowing the generation of an ionic current through the nanopore. The experimental setup was controlled by a patch clamp amplifier (Axopatch 200B, Molecular Device Inc.) and the data acquisition was ensured by an Axon Digidata 1550 A (Molecular Device LLC.) and recorded using Axon pCLAMP 10 (Molecular Device LLC.). To protect the system from any interference, the entire device was placed in a Faraday cage.

2.3. Solid-state nanopore fabrication

The nanopore fabrication process follows similar procedure as previously reported by us [7]. Briefly, starting with a double side polished silicon-on-insulator wafer, composed of an 88 nm thick top silicon layer, a 145 nm thick buried oxide layer and a 300 μm thick silicon substrate. A thin layer of silicon nitride (SiN_x) with a thickness around 30 nm was deposited on both sides of the wafer by means of low-pressure chemical vapor deposition (Koyo Lindberg). Then electron beam lithography (Nanobeam Ltd) and reactive ion etching (RIE) were used to pattern nanoholes in the SiN_x layer on the front side of the wafer. With alignment to the nanoholes, square windows were opened on the rear side of the wafer by photolithography and RIE to enable etching through the silicon substrate in 30% KOH wet etching at 80 °C. The top silicon layer was protected during this step. Finally, the top silicon inside the nanoholes on the front side was etched in 30% KOH at 30 °C. After stripping the buried oxide layer in buffered HF solution, silicon pores were fabricated. After deposition of a thin layer of 2 nm Ti/10 nm Au on top of the silicon pore surface through evaporation (Kurt. J Lesker PVD 75), the chips were ready for further surface modifications.

2.4. Solid-state nanopore surface modification

Following the manufacturing process, the chip was cleaned by plasma treatment (100 W O_2/N_2 for 5 min). Plasma treatment allows a soft and non-destructive cleaning of the chip, unlike a conventional Piranha cleaning [21]. The cleaned gold surface was functionalized by incubating the chip with a solution of cysteamine 5 mM in Milli-Q (MQ, 18.2 MΩ cm^{-1}) water for 2 h. After functionalization, the amine group in cysteamine was further derivatized by reacting with an excess of glutaraldehyde (3% V/V in H_2O). After 1 h incubation, the chip was rinsed with MQ water to eliminate remaining glutaraldehyde. The glutaraldehyde activated chip was used to immobilize casein in the nanopore cavity. Casein was diluted in MQ water (1 mg/mL), and the pH was adjusted to 8 after complete solubilization to optimize the coupling reaction. The sensor substrates were thoroughly cleaned with MQ water to avoid undesired side-reactions after functionalization. Incubation of the chip in an ethanolamine solution followed the immobilization of casein to block remaining glutaraldehyde and limit non-specific absorption. Finally, the chips were rinsed once again with ethanol and MQ water. The reproducibility and the stability of the modification have been investigated and are shown in Fig. S4. The different chips show a good reproducibility after the casein immobilization. The current response remains stable one week after the modification and storage in water, showing no significant desorption of the casein. Since the strong electrical field generated in the nanopore constriction by the voltage bias could significantly influence the enzyme activity, we choose to use end-points measurements instead of real-time measurements for our sensors.

2.5. Nanopore detection of trypsin and gingipain activity

To determine the optimal incubation time for the enzyme, casein functionalized nanopore chips were subjected to 0.1 μg/mL of trypsin in 0.05 mol/L TBS pH 8.0 (0.138 mol/L NaCl; 0.0027 mol/L KCl) for 30, 20, 10 and 5 min at room temperature (RT). Incubation was done using a PDMS well placed on top of the nanopore chip to prevent leakage and ensure the reproducibility of the different incubations. A volume of 50 μL of the enzyme solution was used. The trypsin activity monitoring was performed by incubating the functionalized substrates with different enzyme concentrations (from 0.005 ng/mL to 0.1 μg/mL) in 0.05 mol/L TBS pH 8.0 for 10 min using the same system as previously described. Directly after incubation, the chips were rinsed with MQ water and mounted within the nanopore platform to proceed with the current measurement in 100 mM KCl. The detection of RgpB activity was carried out according to the protocol proposed by Genovis for optimal degradation of proteins by GingisREX. The incubation was performed in 5 M urea in TBS pH 8, 5 mM dithiothreitol (DTT), and 10 mM cysteine. Cysteine was added for reduction and activation of GingisREX. The digestion was performed using 50 μL of the reaction solution placed in a PDMS well on top of the substrate chip for 1 h at 30 °C. After rinsing with MQ water, the measurements were carried out in 100 mM KCl using the nanopore platform.

2.6. Localized surface plasmon resonance (LSPR)

Spherical citrate-covered AuNPs with a diameter of 50 nm (BBI Solutions, USA) were immobilized in 96-well plates (Nunc, transparent, flat, round, pre-treated), according to a protocol previously described [22]. A polyelectrolyte multilayer was adsorbed in the well-plates according to layer-by-layer (LBL) methodology reported by Decher [23]. Polyelectrolyte solutions of polyethylenimine (PEI, Mw 750,000), polystyrene sulfonate (PSS, Mw 75,000), and polyallylamine hydrochloride (PAH, Mw 56,000) were prepared with a concentration of

2 mg/mL in 0.5 M NaCl in MQ water and 70 μL of polyelectrolyte solution was added to each well for 10 min in the order PEI/PSS/-PAH/PSS/PAH with a thorough rinsing of MQ water between each deposition. Finally, 70 μL of the AuNP suspension was added to each well and incubated for 4 h at RT, followed by rinsing with MQ water. Subsequent functionalization of the AuNPs was carried out according to the same protocol as for the nanopores, with minor alterations. Briefly, a self-assembled monolayer of cysteamine (5 mM) dissolved in MQ water was first immobilized, followed by activation with glutaraldehyde (3% V/V in MQ water). Casein, 1 mg/mL (42 μM), was dissolved in MQ water and incubated with the functionalized AuNPs for 2 h in RT. Ethanolamine was used to block and hinder eventual unspecific binding, prior evaluation of trypsin cleavage. Trypsin from bovine serum was dissolved in PBS buffer (140 mM sodium chloride, 2.7 mM potassium chloride and 10 mM phosphate, pH 7.4) to mimic physiological ionic strength and pH and was used for investigating the degradation of the protein film. Trypsin was incubated for 10 min at 37 °C. All incubations steps were followed by rinsing with MQ water (>10 mL per well). The plasmon peak position was monitored after each incubation step. UV−vis absorbance scans 400 − 800 nm was measured using a TECAN Infinite M1000PRO plate reader. Polyelectrolyte layers without AuNPs were measured as a background in the LSPR data and subtracted prior to analysis. Data were fitted to a 9th degree polynomial using Matlab (MATLAB and Statistics Toolbox Release 2017a, The MathWorks, Inc., Natick, Massachusetts, United States) to identify the LSPR peak position. An n-value of n = 3 was applied for all LSPR measurements.

2.7. Null-ellipsometry

Gold film substrates were produced by evaporating a 25 Å Ti adhesion layer followed by 2000 Å of Au on clean (111) silicon wafers in a Baltzers UMS 500 P system. The base pressure was below 10^{-9} Torr, and the evaporation pressure was on the low 10^{-7} Torr scale. The gold surfaces were cleaned in a mixture of 5/7 H_2O, 1/7 H_2O_2 (30%), and 1/7 NH_3 (25%) at ~85 °C for 10 min and thoroughly rinsed with MQ water prior to functionalization. The surfaces were incubated according to the same protocol as for LSPR measurements described above. The protein film thickness was measured using null-ellipsometry on an automatic Rudolph Research AutoEL III ellipsometer with a He−Ne laser operating at 632.8 nm at an angle of incidence of 70°. An optical model based on isotropic optical constants for the protein layer $N_{prot} = n + ik = 1.50$, with n = RI and k = extinction coefficient, was used for the evaluation of the film thickness. Data from five points on each surface were averaged.

2.8. Data handling and statistical analysis

LSPR and ellipsometry data was analyzed in Microsoft Excel 2021 and Matlab (MATLAB and Statistics Toolbox Release R2017a, The MathWorks, Inc., Natick, Massachusetts, United States). LSPR and ellipsometry graphs were visualized with Graph Pad Prism 9 (GraphPad Software, La Jolla California USA).

3. Results and discussion

3.1. Solid state nanopore characterization

Directly after the manufacturing and cleaning process, the nanopore chips were characterized by top-view SEM. Based on analysis of SEM images (Fig. 1 B), the side length of the Si nanopore (truncated pyramid base) was determined to be 30 nm. The green rectangle highlights the area used for this measurement. The presence of the gold layer on the nanopore surface was verified by Energy Dispersive X-Ray Analysis (Fig. S1 and S2). Fig. S3 shows the nanopore chip after gold deposition. To reduce the exposed area of Ti/Au evaporation on the chip surface and tend to a local modification, a shadow mask was used to confine the metals around the free-standing membrane area instead of covering the entire substrate.

Casein was used as a generic protease substrate and was immobilized in cysteamine functionalized nanopores using glutaraldehyde (Fig. 1 C). Casein is a 24 kDa protein that can assemble into colloidal micelles and was shown to effectively block the ionic current through the nanopores (Fig. 1 D). Analysis of the ionic current at each stage of functionalization was carried out (Fig. 1 D). All the measurements presented were performed at a concentration of 100 mM KCl and at potentials between − 150 and 150 mV with a step of 30 mV.

After cleaning of the fabricated nanopores, the ionic current as a function of the applied potential followed a linear dependence. This indicates an ohmic behavior and confirms proper function of the nanopore. Following the formation of the cysteamine self-assembled monolayer, a slight decrease in current intensity was observed, from 2.09 nA to 1.94, at 60 mV. Since cysteamine has a low molecular weight (77.15 g/mol) and short length, the nanopore should only be partially blocked after functionalization, which was confirmed by the small effect on the ionic current. A similar response was recorded after addition of glutaraldehyde, with a decrease from 1.94 nA to 1.39 nA (at 60 mV). In contrast, a very sharp drop to 0.05 nA, was observed after immobilization of casein, reflecting an almost total blocking of the nanopore. The significantly larger size of casein compared to the molecules previously attached to the gold surface can explain this large decrease. Moreover, casein is slightly hydrophobic and has a strong tendency to reduce the water contact angle when immobilized on solid substrates, which can thus lead to additional obstruction of the nanopore. The addition of ethanolamine further reduced the ionic current slightly to 0.03 nA at 60 mV. Ethanolamine was added to deactivate any remaining glutaraldehyde to prevent non-specific adsorption while operating the biosensor.

In parallel, the surface functionalization was confirmed with LSPR using 50 nm AuNPs immobilized in 96 well plates and ellipsometry on planar gold substrates. LSPR data showed a redshift of the LSPR peak position following incubation with cysteamine and glutaraldehyde of $\Delta\lambda_{max} = 0.96$ (0.27) nm and 1.17 (0.12) nm, respectively, mean (SD). The following casein incubation resulted, as expected, and seen previously [24] in a substantial redshift of the peak position of 2.39 (0.15) nm, mean (SD). Addition of ethanolamine resulted in minor blue shift of $\Delta\lambda_{max} = -0.24$ (0.10) nm, mean (SD). Ellipsometry showed a film thickness of 7.90 (0.42) Å following cysteamine coating, 14.7 (2.20) Å after addition of glutaraldehyde layer, 40.0 (2.68) Å after addition of casein and 28.3 (1.85) Å after ethanolamine incubation, mean (SD) (Fig. S4).

3.2. Optimization of trypsin incubation time

To avoid saturating the sensor response and to maximize the dynamic range, the contact time with the sample is critical. In theory, a low concentration of enzymes can digest as much casein as a high concentration of enzyme if the incubation time is sufficiently long, and even result in saturation of the sensor response. However, if the incubation time is shorter than the time required to saturate the response, digestion will be dependent on the enzyme concentration. Incubation time must thus be optimized for the relevant concentration range and activity of the enzyme of interest. The I-V plots resulting from different incubation times of trypsin at 0.1 μg/mL are presented in Fig. 2 A. Fig. 2 B shows the percentage of the ionic current (ΔI) recovered after the incubation of the enzyme. ΔI is defined as follows: $\Delta I = (I_n/I_0) * 100$, where I_n is the current intensity obtained for sample n, and I_0 is the initial ionic current recorded with a clean and unfunctionalized chip.

The degree of casein digestion increased with the incubation time of the enzyme, until reaching sensor signal saturation after 20 min, likely corresponding to complete degradation of the casein layer. The time required to reach saturation was relatively long considering the time required to observe an initial increase in ionic current (1 min under

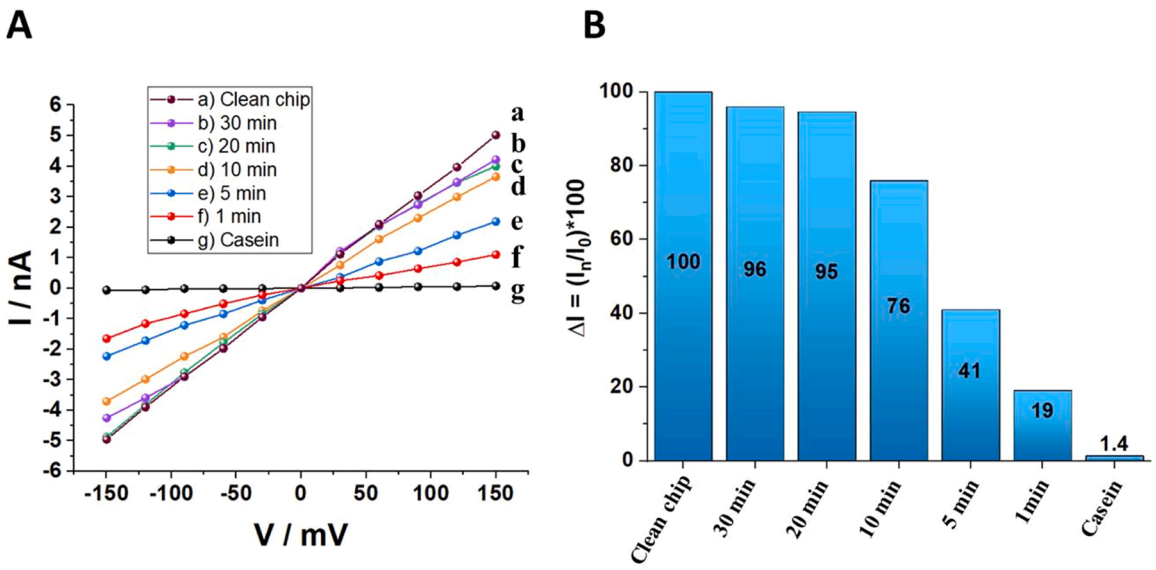

Fig. 2. A) Current−Voltage characteristics at different trypsin incubation times in 100 mM KCl. Trypsin concentration: 0.1 μg/mL. B) The relative current intensity after incubation of trypsin with different digestion times at 60 mV in 100 mM KCl.

optimal conditions) [25] and the high trypsin concentration used (0.1 μg/mL). The slow kinetics likely reflects the steric constrains imposed by the extremely small space confined inside nanopore as that restricts trypsin from accessing the casein. However, already for the shorter incubation times (1 and 5 min) slight but significant increases were seen in the current recovery, from 1.4% after casein immobilization to 19% and 41%, respectively. In comparison, the measured ionic current after 10 min of digestion reached 76% recovery (Fig. 2 B). In order to detect very low enzyme concentrations, it is important to have sufficient sensitivity to be able to distinguish the result of digestion from the baseline values of the current. For incubation times of 1 and 5 min, the increase in the current, although distinguishable from baseline (> 3xSD), remained low considering the high concentration of enzyme used. For 10 min, the percentage recovered was significantly higher while being far from the saturation level of the system and thus seemed optimal with respect to the different times tested. For the rest of the trypsin study, a fixed digestion time (t) of 10 min was consequently used.

3.3. Detection of trypsin

After validation of the experimental protocol and optimization of the incubation time, the detection of different concentrations of trypsin was performed. A range from 0.005 ng/mL to 0.1 μg/mL was investigated, with a fixed incubation time of 10 min. The enzyme was added to the nanopore sensors directly after functionalization and the response was monitored under the same conditions as described above. Each of the concentrations was tested three times on different chips (n = 3) to ensure the reproducibility of the results. The results are shown in Fig. 3 A below.

A gradual increase in current intensity with increasing trypsin concentrations was visible in the selected concentration range, from 0.03 nA to 1.64 nA at a concentration of 0.1 μg/mL at 60 mV. The concentration of 0.1 μg/mL thus reaches a value close to the saturation. The measured current signals could be well fitted with a model described by Lee and all [26]. This model combines Michaelis-Menten kinetics with the Langmuir adsorption model and was developed to describe the activity of hydrolytic enzymes molecules on surface-immobilized substrates. Using this model, the enzymatic reaction can be described as follows:

$$\theta = \frac{[E]}{K_{M'} + [E]}$$

Where θ is the relative surface coverage of the enzyme; E is the concentration of free enzymes at equilibrium (mol/L) and $K_{M'}$ is the apparent Michaelis-Menten constant for enzymes in solution (mol/L).

This model can be applied to the enzymatic reaction in our nanopore sensors to reflect a Michaelis-Menten evolution of the ionic current as a function of the enzyme concentration (Fig. 3 B). Since each individual enzyme on the surface will hydrolyze casein regardless of its environment until saturation, the reaction rate is correlated to θ. The change of the nanopore opening and the ionic current signal can therefore be directly linked to the enzyme concentration via this model. Michaelis-Menten model was used to estimate the apparent Michaelis-Menten constant $K_{M'}$ (9.41 nM). This value is higher than the one found in the literature (0.38 nM) [27], which can be explained by the shape and size of the nanopore, resulting in steric hinderance that reduce accessibility and the rate of the enzymatic reaction.

The enzymatic reaction rate being governed by the casein-trypsin complex formation and the nanopore geometry, our measured electrical signals show a linear evolution of the current as a function of the concentration (Fig. 3 C) over the dynamic concentration range (0.005–100 ng/mL). The experimental data presents a good determination coefficient $R^2 = 0.988$ at the chosen incubation time (t = 10 min). The linearity in this concentration range facilitates quantitative determination of enzyme concentration.

The LOD for detection of trypsin was 0.005 ng/mL (0.2 pM) and the sensor displayed a dynamic range covering five orders of magnitude (0.005–0.1 μg/mL). For comparison, most of the biosensors discussed in the literature achieve LOD values ranging from 0.1 to 1 ng/mL over a similar dynamic range [28–30]. The high performance observed here can primarily be due to the extremely sensitive ionic current measurement using the nanopore system. Each change at its interface, and therefore the digestion of a very small quantity of substrate by the enzyme, can thus be detected.

Another important factor, apart from the intrinsic performance of the biosensor, is the specificity of the molecular architecture created with respect to trypsin. The response of the biosensor when exposed to trypsin in the presence of inhibitors as wells as non-specific adsorption of proteins was studied. These results are presented in Fig. 3 D. The recovery in ionic current after incubation with trypsin (0.1 μg/mL) in the presence

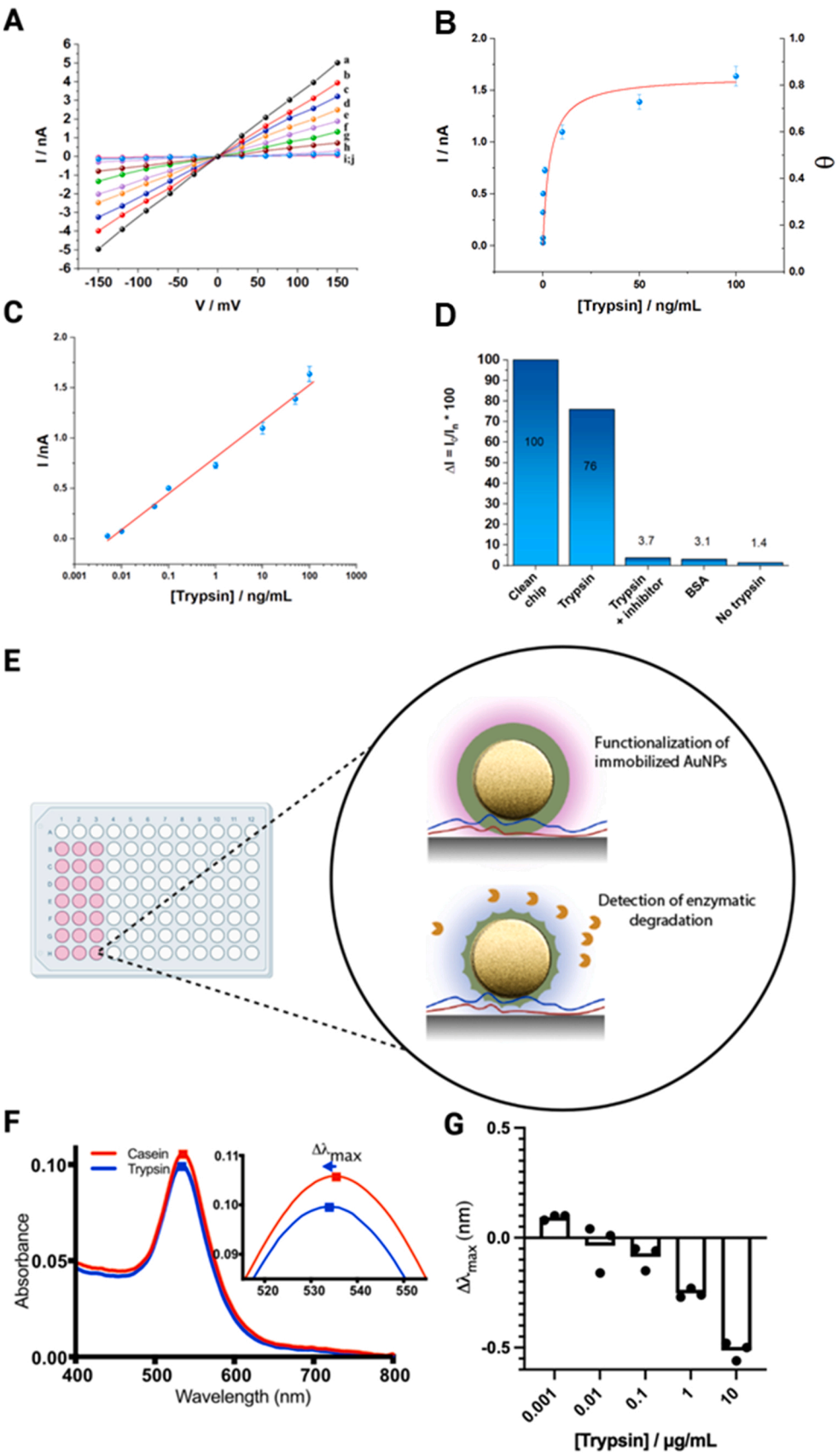

Fig. 3. A) Current−Voltage characteristics at different trypsin concentrations in 100 mM KCl. From bottom to top: 0, 0.005, 0.01, 0.05, 0.1, 1, 10, 50 and 100 ng/mL. B) Evolution of the ionic current as a function of the trypsin concentration and the modeled evolution of the relative surface coverage of trypsin (red line). C) Evolution of the ionic current as a function of the logarithm of the trypsin concentration. Experimental data obtained on 3 different electrodes (dots) and linear regression (line) are presented. Linear regression: $y = 0.156\ \ln(x) + 0.8089$; $R^2 = 0.988$. D) The relative current intensity after incubation of different biomolecules at 60 mV in 100 mM KCl. E) Schematic overview of LSPR experimental process. Degradation of casein immobilized on the AuNPs by proteases. Created with BioRender.com F) UV–vis spectra before and after enzymatic degradation (inset represents in-zoom of peak position). G) LSPR response of trypsin on coated AuNPs (spherical 50 nm). LSPR peak position shifts after trypsin incubation for 10 min. LOD = 1 µg/mL. $p < 0.05$ (Kruskal-Wallis).

of Soybean Trypsin Inhibitor (0.1 μg/mL) was only 1.7%. In contrast, trypsin without inhibitor resulted in a 75% increase in ionic current under the same conditions. Furthermore, casein is widely used to block unspecific adsorption of proteins to substrates in various bioanalytical assays. The effect of unspecific adsorption of bovine serum albumin (BSA, 0.1 μg/mL) on the sensor surface was investigated and resulted in a slight increase in ionic current of 2.3%, potentially as a result of surface exchange reaction between casein micelles and BSA.

3.4. Detection of trypsin with LSPR

To further corroborate the results of the nanopore data, the same interaction was investigated using LSPR. A concentration-dependent degradation of the protein film by trypsin was observed, with an increase in degradation with increasing trypsin concentration, corresponding to a change in the refractive index near the sensor surface (Fig. 3 G). The LOD of this setup was determined to be 1 μg/mL. The blueshifts shown are modest, but significant (Kruskal-Wallis $p < 0.05$). More pronounced blueshifts have been shown in previously reported similar setups [24]. Since LSPR has a relatively low sensing depth (typically < 20 nm), the increase in distance between the AuNPs and the casein caused by the casein immobilization strategy used here is expected to decrease the LOD. Moreover, since LSPR detects refractive index changes, a larger proportion of the immobilized casein must be degraded to accomplish a significant sensor response, compared to the nanopore sensor where a relatively large increase in ion current can be observed already at very low concentrations of proteases. The decrease in thickness of the surface coating by trypsin was further investigated using null-ellipsometry. Trypsin (10 μg /mL) reduced the film thickness from 28.3 (1.85) Å to 23.9 (4.32) Å, mean (SD), corresponding to a decrease of 4.4 Å (Fig. S4).

3.5. Gingipains assay in urea solution

Once the protocol was clearly established after studying the model case with trypsin, tests were carried out on the detection of gingipain enzymes. Gingipains are trypsin-like cysteine endopeptidases, secreted by *P. gingivalis*. Arginine specific gingipains (Rgp) cleave peptides on the C-terminal of arginine. Whereas RgpA, like lysine specific gingipain (Kgp), have an adhesion domain in addition to the proteolytic domain, RgpB has solely a proteolytic domain. Here, RgpB was allowed to degrade the casein in the nanopores during 1 h at 30 °C in the presence of 5 M urea, 5 mM DTT and 10 mM cysteine, pH 8.5. As controls, other incubations were carried out in parallel with a non-activated form of RgpB and in urea without RgpB. The semi-logarithmic evolution of the current as a function of the concentration after digestion is shown in Fig. 4 A. Fig. 4 B shows the recovery of the ionic current (ΔI) after enzyme incubation with I_0 being the ionic current recorded on a clean chip prior to modification.

After incubation of the activated form of RgpB, an increase in the intensity of the ionic current was observed that also increased with enzyme concentration, from 0.24 nA at 1 ng/mL to 0.57 nA at 0.1 μg/mL. A distinct difference amidst these results and the trypsin model can be observed with respect to the detection range and the correlation between experimental and theoretical data. The LOD reached for gingipains is indeed higher, with 1 ng/mL (0.02 nM) against 0.005 ng/mL (0.2 pM) for trypsin. This difference is likely both a result of the higher molecular weight of RgpB (50 kDa) [31] and the higher selectivity of RgpB compared to trypsin. Beta-casein has only 4 arginine residues, making cleavage by Rgp less likely and less efficient compared to trypsin. In addition, RgpB, lacks the adhesion domain that is present in other gingipain subtypes (Kgp and RgpA), which promotes association of enzyme to both other proteins and surfaces. With respect to the relative ionic current intensity, Fig. 4 B shows a restitution of 27% of the initial current after incubation with 0.1 μg/mL of activated RgpB. The intensity is thus lower than that observed for the digestion of casein by trypsin in a controlled medium, further indicating that more of the casein remains after cleavage by RgpB. However, the sensor signal is still significantly higher than the ionic current recorded for the non-activated enzyme (7%) and for the test carried out in the presence of urea without enzyme (2.5%), attesting to the specificity of the system. Moreover, the LOD is substantially lower than the concentrations of Rgp observed in patients suffering from severe chronic periodontitis (≤1.5 μM) [32] and also below the concentrations for total protease activity in patients with peri-implantitis [33] and gingivitis [34].

Thus, despite a shorter dynamic range than for trypsin, the biosensor presented remains interesting in terms of ease of operation, speed of detection and selectivity for the detection of gingipain. There is no doubt

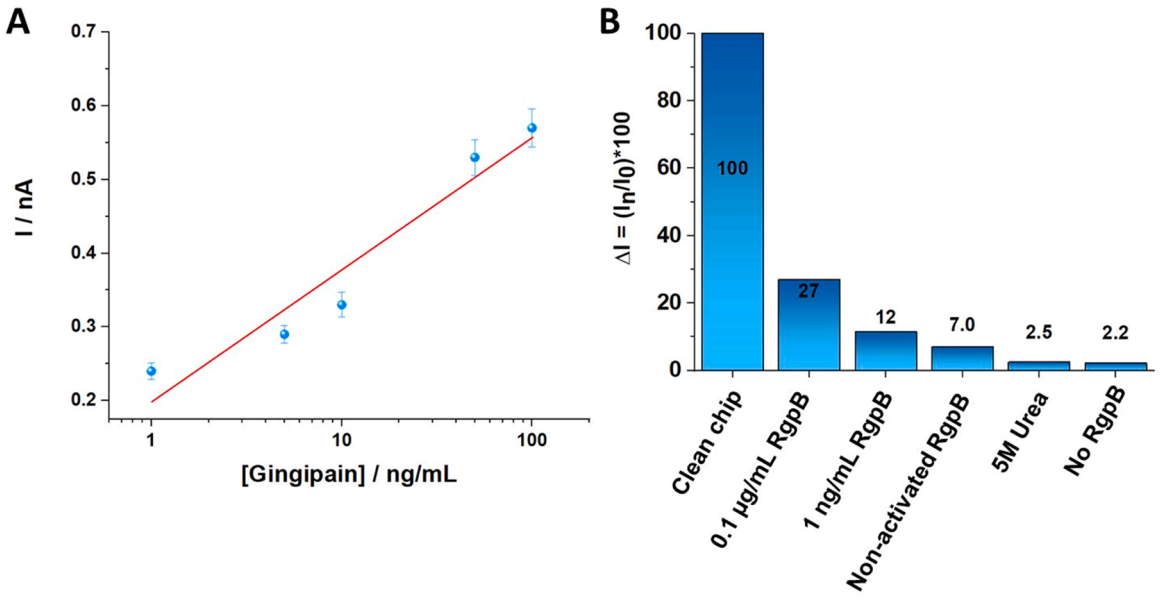

Fig. 4. A) Evolution of the ionic current as a function of the logarithm of the gingipain concentration at 60 mV. Experimental data (dots) and linear regression (line) are presented. Linear regression: $y = 0.0779 \ln(x) + 0.1983$; $R^2 = 0.931$. B) The relative current intensity after incubation of activated gingipains at different concentrations and after incubation of a non-activated form of gingipain at 60 mV in 100 mM KCl.

that a more in-depth study of this complex system will allow further detection of gingipain but also of other potential enzymes.

4. Conclusion

A novel sensor strategy, based on casein-functionalized solid-state nanopores for detection of proteolytic activity, was demonstrated. Proteolytic degradation of casein, immobilized in the nanopores, restored the ionic current. The LOD for detection of trypsin was 0.005 ng/mL (0.2 pM) and the sensor showed a dynamic range spanning over 5 orders of magnitude. Trypsin degradation of the protein film was further confirmed using LSPR and ellipsometry. The LOD for detection of RgpB was 1 ng/mL with a 27% recovery of the signal at 0.1 μg/mL, indicating that the sensitivity and dynamic range are relevant for clinical diagnosis of periodontitis. This promising sensor technology show a potential for detection of periodontal disease and could possible also be tuned for detection of other proteases and their related infections.

CRediT authorship contribution statement

Q.P. did the surface functionalization, sensing measurements, data analysis and paper writing. **A.S.** did LSPR and null-ellipsometry measurements, contributed to data analysis and paper writing. **S.Z.** fabricated the nanopore devices, contributed to data analysis and paper writing. **Q.H. and F.L.** contributed to the device fabrication. **D.A. and Z. Z.** secured the funding, supervised the project, contributed to data analysis and paper writing.

Declaration of Competing Interest

The authors declare that they have no known competing financial interests or personal relationships that could have appeared to influence the work reported in this paper.

Acknowledgements

This work was supported by the Swedish Strategic Research Foundation (SSF FFL15-0174 and FFL15-0026), the Swedish Research Council (VR 2019-04690, VR 2017-04475 and VR 2016-04874), and the Swedish Cancer Foundation (CAN 2017/430), and the Wallenberg Academy Fellow Program (KAW 2020.0190 and KAW 2016.0231).

Appendix A. Supporting information

Supplementary data associated with this article can be found in the online version at doi:10.1016/j.snb.2022.132209.

References

[1] I.L.H. Ong, K.L. Yang, Recent developments in protease activity assays and sensors, Analyst 142 (2017) 1867–1881.
[2] D.F. Kinane, P.G. Stathopoulou, P.N. Papapanou, Periodontal diseases, 2017, Nat. Rev. Dis. Prim. 31 (3) (2017) 1–14.
[3] B.L. Pihlstrom, B.S. Michalowicz, N.W. Johnson, Periodontal diseases, Lancet 366 (2005) 1809–1820.
[4] V.I. Haraszthy, J.J. Zambon, M. Trevisan, M. Zeid, R.J. Genco, Identification of periodontal pathogens in atheromatous plaques, J. Periodontol. 71 (2000) 1554–1560.
[5] S.S. Dominy, et al., Porphyromonas gingivalis in Alzheimer's disease brains: evidence for disease causation and treatment with small-molecule inhibitors, Sci. Adv. 5 (2019).
[6] E.F. Carrizales-Sepúlveda, A. Ordaz-Farías, R. Vera-Pineda, R. Flores-Ramírez, Periodontal disease, systemic inflammation and the risk of cardiovascular disease, Hear Lung Circ. 27 (2018) 1327–1334.
[7] D. Liccardo, et al., Periodontal disease: a risk factor for diabetes and cardiovascular disease, Int. J. Mol. Sci. 20 (2019) 1414.
[8] M. Sochocka, et al., Association between periodontal health status and cognitive abilities. The role of cytokine profile and systemic inflammation, Curr. Alzheimer Res. 14 (2017).
[9] Y. Guo, K.A. Nguyen, J. Potempa, Dichotomy of gingipains action as virulence factors: from cleaving substrates with the precision of a surgeon's knife to a meat chopper-like brutal degradation of proteins, Periodontology 54 (2010) 15–44.
[10] R.E. Fitzpatrick, L.C. Wijeyewickrema, R.N. Pike, The gingipains: scissors and glue of the periodontal pathogen, Porphyromonas gingivalis 4 (2009) 471–487. ⟨https://doi.org/10.2217/fmb.09.18⟩.
[11] R. Antiochia, Developments in biosensors for CoV detection and future trends, Biosens. Bioelectron. 173 (2021), 112777.
[12] W. Shi, A.K. Friedman, L.A. Baker, Nanopore sensing, Anal. Chem. 89 (2016) 157–188.
[13] Y. He, M. Tsutsui, Y. Zhou, X.-S. Miao, Solid-state nanopore systems: from materials to applications, 2021, NPG Asia Mater. 131 (13) (2021) 1–26.
[14] Q. Chen, Z. Liu, Fabrication and applications of solid-state nanopores, Sensors 19 (2019).
[15] W. Shi, A.K. Friedman, L.A. Baker, Nanopore sensing, Anal. Chem. 89 (2017) 157–188.
[16] C. Dekker, Solid-state nanopores, Nat. Nanotechnol. 2 (2007) 209–215.
[17] S. Zeng, C. Wen, P. Solomon, S.-L. Zhang, Z. Zhang, Rectification of protein translocation in truncated pyramidal nanopores. Nat. Nanotechnol. 14.
[18] C. Wen, S. Zeng, S. Li, Z. Zhang, S.-L. Zhang, On rectification of ionic current in nanopores, Anal. Chem. 91 (2019) 14597–14604.
[19] W. Rick, Trypsin, Methods Enzym. Anal. (1974) 1013–1024, https://doi.org/10.1016/B978-0-12-091302-2.50099-2.
[20] T. Imamura, The role of gingipains in the pathogenesis of periodontal disease, J. Periodontol. 74 (2003) 111–118.
[21] J.K. and, P.A. Rowntree, Gold film surface preparation for self-assembled monolayer studies, Langmuir 23 (2006) 509–516.
[22] R.I. Nooney, O. Stranik, C. McDonagh, B.D. MacCraith, Optimization of plasmonic enhancement of fluorescence on plastic substrates, Langmuir 24 (2008) 11261–11267.
[23] G. Decher, Fuzzy nanoassemblies: toward layered polymeric multicomposites, Science 277 (1997) 1232–1237.
[24] D. Aili, et al., Protein-functionalized gold nanoparticles as refractometric nanoplasmonic sensors for the detection of proteolytic activity of porphyromonas gingivalis, ACS Appl. Nano Mater. 3 (2020) 9822–9830.
[25] E.M. Srokowski, K.A. Woodhouse, Decellularized scaffolds, Compr. Biomater. 2 (2011) 369–386.
[26] H.J. Lee, A.W. Wark, T.T. Goodrich, S. Fang, R.M. Corn, Surface Enzyme Kinetics for Biopolymer Microarrays: A Combination of Langmuir and Michaelis-Menten Concepts, 2005. doi:⟨10.1021/la046822h⟩.
[27] S. Spagnolo, E.S. Muckley, I.N. Ivanov, T. Hianik, Analysis of trypsin activity at β-casein layers formed on hydrophobic surfaces using a multiharmonic acoustic method, Analyst 147 (2022) 461–470.
[28] C.X. Zhuo, L.H. Wang, J.J. Feng, Y.D. Zhang, Label-free fluorescent detection of trypsin activity based on DNA-stabilized silver nanocluster-peptide conjugates, Sensors 16 (2016) 1477.
[29] L. Hu, et al., Highly sensitive fluorescent detection of trypsin based on BSA-stabilized gold nanoclusters, Biosens. Bioelectron. 32 (2012) 297–299.
[30] S. Xu, et al., A fluorescence resonance energy transfer biosensor based on carbon dots and gold nanoparticles for the detection of trypsin, Sens. Actuators B Chem. 273 (2018) 1015–1021.
[31] L. Jia, et al., Pathogenesis of important virulence factors of Porphyromonas gingivalis via toll-like receptors, Front. Cell. Infect. Microbiol. 9 (2019) 262.
[32] A. Guentsch, et al., Comparison of gingival crevicular fluid sampling methods in patients with severe chronic periodontitis, J. Periodontol. 82 (2011) 1051–1060.
[33] J. Neilands, et al., Bacterial profiles and proteolytic activity in peri-implantitis versus healthy sites, Anaerobe 35 (2015) 28–34.
[34] C.M.S. Figueredo, A. Gustafsson, Protease activity in gingival crevicular fluid, J. Clin. Periodontol. 25 (1998) 306–310.

Quentin Palomar has joined the group "Biosystèmes Electrochimiques & Analytiques" (BEA) headed by Dr. Serge Cosnier at the DCM unit of the University of Grenoble as a Ph.D. student in 2014. In 2017, he completed his Ph.D. in biosensor design entitled: Integration of nanostructured materials in the design and realization of label-free biosensors for detection of targets of interest. In 2018, he joined Professor Zhen Zhang's group as a postdoctoral researcher. His current work focuses on the design of biosensors based on silicon nanopore and on electrochemical detection of biomolecules.

Anna Svärd is a doctoral student in biomedicine at the School of Medical Sciences, Örebro University, Sweden and at the Laboratory of Molecular Materials at Linköping University, Sweden. Anna graduated as DDS from the Sahlgrenska Academy in Gothenburg (2011) and has a M.Sc. in Experimental and Medical Sciences from Linköping University, Sweden (2016). The Ph.D. projects focuses on detection and inhibition of gingipain enzymes in periodontal disease.

Qitao Hu received the B.S. degree (2015) from University of Science and Technology of China. From 2016–2021, he was a Ph.D. student at the group of Prof. Zhen Zhang at solid-state electronics at Uppsala University. His Ph.D. study was focused on fabrication of silicon nanoelectronic devices and exploration of their applications in ion sensing area. Currently, he is a postdoctoral researcher at Prof. Zhang's group, and he is studying the applications of silicon nanosensors in single-molecule analysis and gas detection.

Funing Liu studied self-assembled polymers in the Optical Polymer Laboratory (supervisor: Professor Gang Zou) and got the B.Sc. and M.Sc. degree at University of Science and

Technology of China (USTC) in 2016 and 2019. She focused on the fabrication of biosensors based on one-dimensional polydiacetylene (PDA) microtube. The thesis is entitled as "Sensitive discrimination of single nucleotide variants using a PDA microtube waveguide platform with heterogeneous CHA amplification and competitive inhibition strategy." She joined Professor Zhen Zhang's group as a Ph.D. student in 2021. Her current work is the single molecule detection using Si nanocavity.

Shuangshuang Zeng was born in China and received his bachelor degree from University of Science and Technology of China in 2015. In 2020, he earned his Ph.D. degree with a research topic of solid-state nanopore fabrication and applications from Uppsala University, Sweden. He then proceeded with postdoctoral studies in the same group for one and half years.

Prof. Daniel Aili is professor of Molecular Physics at Linköping University (LiU), Sweden. He has a Ph.D. in Sensor science (2008) and an M.Sc. in Engineering Biology (2003) from LiU. After postdocs at Dept. of Materials and Institute of Biomedical Engineering, Imperial College London, UK, and at the School of Materials Science and Engineering at NTU, Singapore, he returned to LiU in 2011 to set up the Laboratory of Molecular Materials. Aili is a Wallenberg Academy Fellow and has received the AkzoNobel Nordic Prize for Surface and Colloid Chemistry, Ingvar Carlsson Award and The Arnbergska Prize from The Royal Swedish Academy of Sciences.

Prof. Zhen Zhang is currently a professor in electronics at the Angstrom Laboratory, Uppsala University, Sweden and an adjunct researcher with IBM T. J. Watson Research Center, Yorktown Heights, NY. Before joining Uppsala University as a tenure track assistant professor in Aug. 2013, he was a postdoctoral research fellow (2008–2010) then a Research Staff Member (2010–2013) at IBM T. J. Watson Research Center. Dr. Zhang received his Ph.D. degree from the Royal Institute of Technology (KTH), Sweden in 2008. He got the M.Sc. degree at Shanghai Institute of Ceramics, Chinese Academy of Sciences in 2003 and the B.Sc. degree at University of Science and Technology of China (USTC) in 2000.